Journal of Hazardous Materials xxx (2011) xxx–xxx

Contents lists available at ScienceDirect

Journal of Hazardous Materials

journal homepage: www.elsevier.com/locate/jhazmat

Size distribution and chemical composition of metalliferous stack emissions in the San Roque petroleum refinery complex, southern Spain

A.M. Sánchez de la Campa[a,*], T. Moreno[b], J. de la Rosa[c], A. Alastuey[b], X. Querol[b]

[a] Estación Experimental del Zaidín, CSIC, C/Profesor Albareda 1, E18008 Granada, Spain
[b] Institute of Environmental Assessment and Water Research IDÆA, CSIC, C/Jordi Girona, 18-26, 08034 Barcelona, Spain
[c] Associate Unit CSIC – University of Huelva "Atmospheric Pollution", Center for Research in Sustainable Chemistry (CIQSO), University of Huelva, E21071 Huelva, Spain

ARTICLE INFO

Article history:
Received 29 November 2010
Received in revised form 3 March 2011
Accepted 29 March 2011
Available online xxx

Keywords:
Atmospheric emissions
Trace metals
Petroleum refinery
Bay of Algeciras

ABSTRACT

We demonstrate that there is great variation in the size range and chemical composition of metalliferous particulate matter (PM) present within petrochemical complex chimney stacks. Cascade impactor PM samples from seven size ranges (17, 14, 5, 2.5, 1.3, 0.67, and 0.33 μm) were collected from inside stacks within the San Roque complex which includes the largest oil refinery in Spain. SEM analysis demonstrates the PM to be mostly carbonaceous and aluminous fly ash and abundant fine metalliferous particles. The metals with the most extreme concentrations averaged over all size ranges were Ni (up to 3295 μg m^{-3}), Cr (962 μg m^{-3}), V (638 μg m^{-3}), Zn (225 μg m^{-3}), Mo (91 μg m^{-3}), La (865 μg m^{-3}), and Co (94 μg m^{-3}). Most metal PM are strongly concentrated into the finest fraction (<0.33 μm), although emissions from some processes, such as purified terephthallic acid (PTA) production, show coarser size ranges. The fluid catalytic cracking stack shows high concentrations of La (>200 μg m^{-3} in $PM_{0.67–1.3}$), Cr and Ni in a relatively coarse PM size range (0.7–14 μm). Our unique database, directly sampled from chimney stacks, confirms that oil refinery complexes such as San Roque are a potent source of a variety of fine, deeply inhalable metalliferous atmospheric PM emissions.

1. Introduction

A variety of gaseous pollutants (e.g. SO_2, CO, NO_x, and H_2S), hydrocarbons, fly ashes and metalliferous particles are released into the atmosphere during the refining of crude oil and processing of its downstream products in petrochemical complexes [1]. Despite atmospheric emissions in Europe and North America being under greater governmental control than in other continents, petroleum refineries are still major pollution hot spots which inevitably impact on local ecosystems [2,3] and human health [4], influencing not only workers [5,6] but also surrounding populations (e.g. [7–9]).

This study deals with the size distributions and chemical characterisation of particulate matter emitted by different chimney stacks in the San Roque petrochemical refinery complex, which is situated on the north side of the Bay of Algeciras in southern Spain (Fig. 1). The Bay of Algeciras is a well documented industrial pollution hot spot [10], with relatively high concentrations of metals such as Ni, V, Cr and La in PM_{10} and $PM_{2.5}$ being attributed to both industrial and shipping [11–14]. The Gibraltar Strait is accessed by around 80,000 ships per year, leaving or entering the Mediterranean. Abnormally high values of La compared to heavier lanthanoids (e.g. La/Ce > 1) implicate the San Roque FCC refinery as a point source for some of these metals [14]. In the present paper we go directly to this source and report on PM samples collected from inside the chimney stacks of the San Roque refinery. To our knowledge this is the first time that detailed physical and chemical characterisation of such samples has been published.

2. Study location

The San Roque refinery complex lies in a densely populated area that includes two major towns, Algeciras (120,000 inhabitants) and La Linea (65,000 inhabitants), which lie 9 km apart and diametrically opposite each other on the SW and NE sides of the bay (Fig. 1). The refinery has a capacity of 240,000 b/d (annual distillation of 12×10^6 tonnes of oil), making it the largest in Spain, and produces all types of fuel (propane, butane, gasoline, aviation fuel diesel and fuel oils). Adjacent to the main refinery plants (which include a fluid catalytic converting facility), further petrochemical processing areas with chimney stacks include those of the Guadarranque and Lubrisur plants (Fig. 1), both of which were also incorporated in this study.

Within the refinery there are two distillation units (Crude I and Crude III), these being characterised by the presence of distillation column towers operating at atmospheric pressure, where crude oil

* Corresponding author. Tel.: +34 959 219855; fax: +34 959 219810.
E-mail address: ana.sanchez@pi.uhu.es (A.M. Sánchez de la Campa).

0304-3894/$ – see front matter © 2011 Published by Elsevier B.V.
doi:10.1016/j.jhazmat.2011.03.104

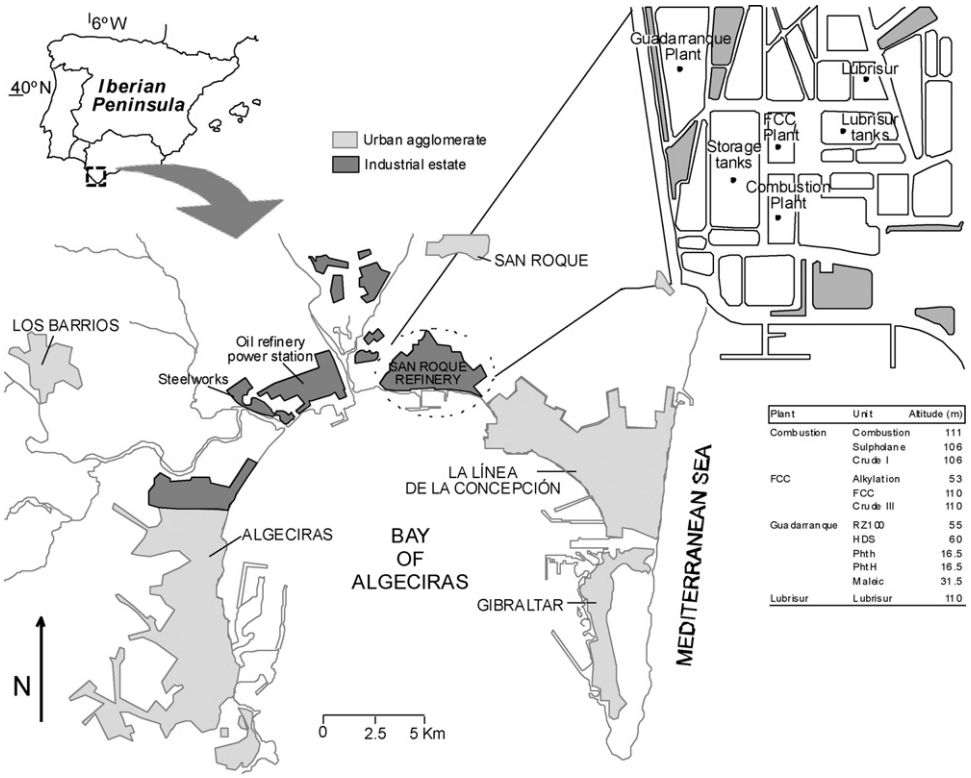

Fig. 1. Generalised map of the Bay of Algeciras and location of Petrochemical plant and San Roque refinery. Details of the refinery and the altitude of stacks samples have been added.

is heated to the temperature of 379 °C in order to obtain a number of hydrocarbon compounds of different boiling-point ranges. These compounds are separated and treated further to produce gases (butane, propane), gasoline (from naphtha), aviation fuel, and fuel oils. The residual heavy hydrocarbons ("atmospheric bottoms") are further distilled under vacuum, mixed with heavy fuel oil and passed to the Fluid Catalytic Cracking (FCC) plant to be cracked into lighter compounds and processed to form gasoline. The cracking is achieved using a catalyst enriched in Rare Earth Elements (especially La), which can be emitted to the atmosphere during the process [15,16]. The lighter hydrocarbons produced in the FCC plant area are transformed into gasoline after treatment in an alkylation unit. In the Guadarranque plant, other refining processes produce basic materials for the petrochemicals industry, such as purified terephthalic acid (PTA) which is used in the manufacturing of polyester. Finally, the Lubrisur plant, which is located at the north end of the petrochemical complex, produces bases for lubricants and other blended products.

3. Methodology

Twelve chimney stack's PM samples in the San Roque refinery complex were obtained using the University of Washington Mark III cascade impactor [17] for analysis of particulate size distribution. Of the 12 stacks sampled, 3 were in the area referred to as the combustion plant, 3 in the area of the FCC plant, 5 in the Guadarranque plant, and 1 in the Lubrisur plant (Fig. 1). Samplers in the combustion plant were positioned at over 100 m above ground level within chimneys venting emissions from fuel oil combustion (111 m), from the Crude I distillation unit (106 m), and from a sulpholane plant (106 m) where aromatic hydrocarbons are extracted from hydrocarbon mixtures. The sampled chimney stacks in the FCC plant area included the FCC unit itself (110 m), the Crude III distillation unit (110 m), and the alkylation unit (53 m). Within the Guadarranque plant samples were taken from emissions from the RZ-100 unit (55 m: catalytic reforming of light naphtha), the HDS unit (60 m: catalytic removal of S from naphtha), and emissions during the production of PTA (Phthalic 1 and 2: 16.5 m) and maleic anhydride (Maleic: 31.5 m). The single sample from the Lubrisur plant was taken from a height of 110 m in the chimney.

Seven effective cut off stage diameters (17, 14, 5, 2.5, 1.3, 0.67, and 0.33 μm) and back up (<0.33 μm) were used. Quartz microfiber filters (47 mm filter diameter and 0.45 μm pore diameter) were used for 10-min individual – isokinetic cascade impactor sampling.

Once the mass levels of PM_{10} were obtained by weighing the filters using standard procedures (T = 20 °C and Relative Humidity = 50%), a half fraction of each of them was submitted to an acid digestion (0.25 ml HNO_3: 0.5 ml HF: 0.25 ml $HClO_4$) following the modified method proposed by Querol et al. [18], for the analysis of 43 trace elements (Li, Be, Sc, V, Cr, Co, Ni, Cu, Zn, Ga, Ge, As, Se, Rb, Sr, Y, Zr, Nb, Mo, Cd, Cs, Ba, La, Ce, Pr, Nd, Sm, Eu, Gd, Tb, Dy, Ho, Er, Tm, Yb, Lu, Ta, W, Tl, Pb, Bi, Th, y U) by means of ICP-MS (HP 4500®).

Three multi-elemental solutions Spec® 1 (rare earth elements, REE), Spec® 2 (alkalis, earth alkalis, and metals) and Spec® 4 (Nb) were used to construct an external calibration curve. The average precision and the accuracy fall for most of the elements under the normal analytical errors (in the range of 5–10%), and were controlled by repeated analysis of NBS-1633a (fly ash) reference material. The lower detection limit (LDL) for the most of elements in solution was 0.01 ppb.

The size, morphology and chemical composition of individual particles were evaluated by scanning electron microscopy with energy dispersive spectrometer (SEM-EDS). The particles were analysed individually using a LINK-ISIS energy-dispersive spectrometer mounted on a SEM (JEOL-JSM5410). Conditions were fit to 15 kV accelerating voltage and 100 s of effective counting time. Matrix corrections were made following the ZAF procedures, using a combination of silicate, oxides and pure metals as stan-

Please cite this article in press as: A.M. Sánchez de la Campa, et al., Size distribution and chemical composition of metalliferous stack emissions in the San Roque petroleum refinery complex, southern Spain, J. Hazard. Mater. (2011), doi:10.1016/j.jhazmat.2011.03.104

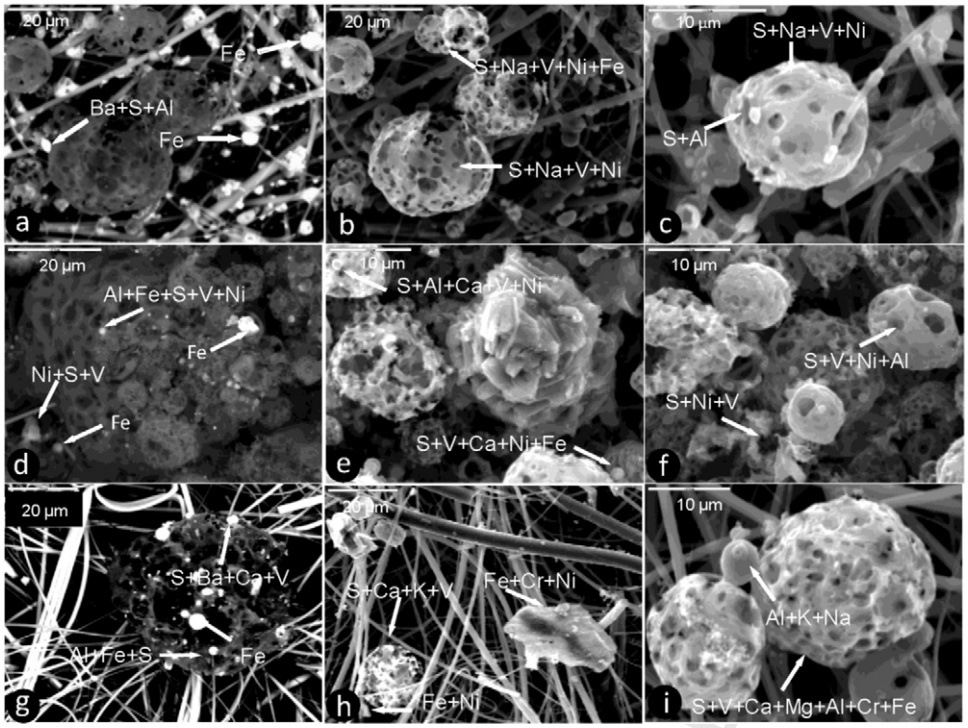

Fig. 2. Secondary and Back-scattered electron images (SEI and BSEI) of representative particles from emissions stacks showing coarse porous individual particles with spherical morphology and fine particles of variable composition.

dards (wollastonite for Ca and Si, jadeite for Na, orthoclase for K, corundum for Al, periclase for Mg, metallic Fe and Ti for Fe and Ti).

4. Results

The PM samples collected from the San Roque chimney stacks are predictably rich in fly ash particles, and representative stack samples examined and analysed by SEM-EDS are shown in Fig. 2. In the combustion sample, coarse (>20 μm) carbonaceous porous fly ash particles are dominant (around 75%). In addition there are aluminous fly ashes (>2 μm), typically rounded to subrounded hollow and composed of Al ± Fe ± Ni ± V. Fine (<2 μm) and ultrafine particles composed of S ± Al ± Fe ± Mg ± Ti ± Ni ± V ± Na ± Ba are seen adhered to the surface of the coarser PM. Similar fly ash particles dominate the PM samples from the FCC and Guadarranque plants, with the largest particles being observed in the HDS unit (>40 μm). Gypsum particles with rose habit are present at the alkylation unit particles (Fig. 2e). The FCC unit sample shows smaller carbonaceous particles (<2 μm) than those from the other units, whereas the particles from the RZ100 unit are irregular in shape, coarse grained (around <30 μm), and composed of Fe + Cr + Ni ± Al.

One of the most striking features of the SEM images is the very fine size of most metalliferous particles. The elemental mass concentrations of ten of the most common metals are provided in Table 1 and displayed graphically in Figs. 3–6. The three samples taken from units in the combustion plant (combustion, sulpholane and Crude I) show a unimodal pattern of ultrafine size PM in the combustion and sulpholane units, and of coarse size in the Crude I unit. Unimodal profiles in the finest (<0.33 μm) size fraction with maximum concentrations of V + Cr + Co + Ni + Cu + Zn + Mo + Pb were observed in the combustion and sulpholane samples, and Cu + Pb in the Crude I sample. Another unimodal size distribution is observed in the fine-coarse size range in La (combustion and Sulpholane) and Ce at the Combustion sample. Only Crude I sample exhibited a bimodal grain size profile (ultrafine and coarse modes), together with the maximum concentration of V + Co + Ni + Zn + La. Finally, a fine unimodal size distribution (0.33–0.67 μm, in all three samples) was observed. The highest metal concentrations in flue gas emissions of this plant were reached by Ni (104 μg m^{-3}), V

Table 1
Geochemical profile of main production plants and units in San Roque refinery.

Production plant	Unit	Very fine (<0.67 μm)	Fine to coarse (0.67–5 μm)	Very coarse (5–17 μm)
Combustion	Combustion	V + Cr + Co + Ni + Cu + Zn + Mo + Pb	La + Ce	–
	Sulpholane		La	–
	Crude I	Cu + Pb and V + Co + Ni + Zn		V + Co + Ni + Zn
FCC	Alkylation	V + Cr + Co + Ni + Cu + Mo		
	FCC	–	V + Cr + Co + Ni + Cu + Mo and La + Ce + Zn	La + Ce + Zn
	Crude III	–	V + Co	Cr + La + Ce
Guadarranque	RZ100	V + Cr + Co + Ni + Cu + Zn + Mo + La + Ce + Pb	–	–
	HDS	Cr + Co + Ni + Cu + Mo + Pb	–	La + Ce
	Phthalic h	Zn + Mo + Ce + Pb and Cr + Co + Ni + Cu	–	La and Cr + Co + Ni + Cu
	Phthalic H	Cu and Cr	–	Zn + La + Ce and Cr
	Maleic	V + Pb	–	Cr + Co + Ni + Cu + Zn + Mo + La + Ce and V + Pb
Lubrisur	Lubrisur	V + Co + Ni	–	V + Co + Ni and La + Ce

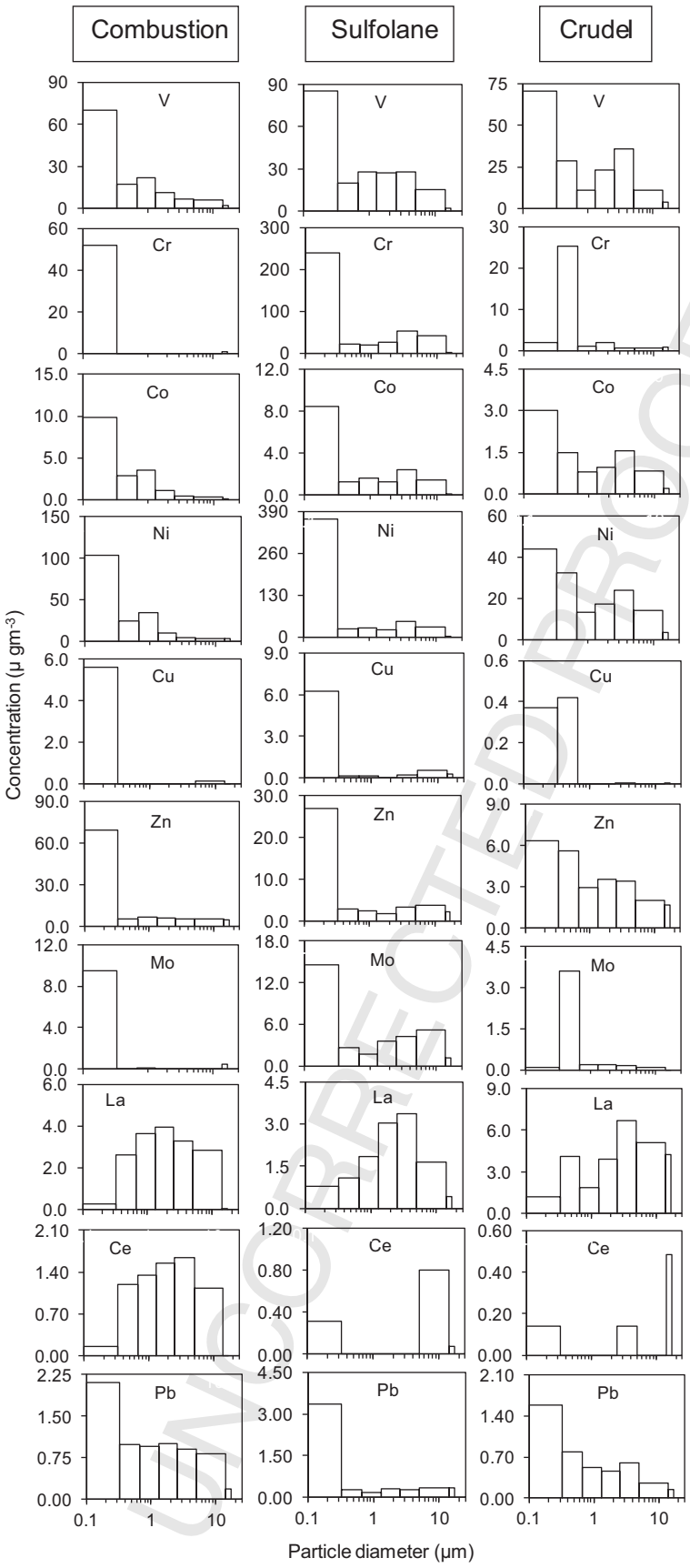

Fig. 3. Concentration and particle size distribution from combustion, sulpholane and Crude I process of combustion plant.

Please cite this article in press as: A.M. Sánchez de la Campa, et al., Size distribution and chemical composition of metalliferous stack emissions in the San Roque petroleum refinery complex, southern Spain, J. Hazard. Mater. (2011), doi:10.1016/j.jhazmat.2011.03.104

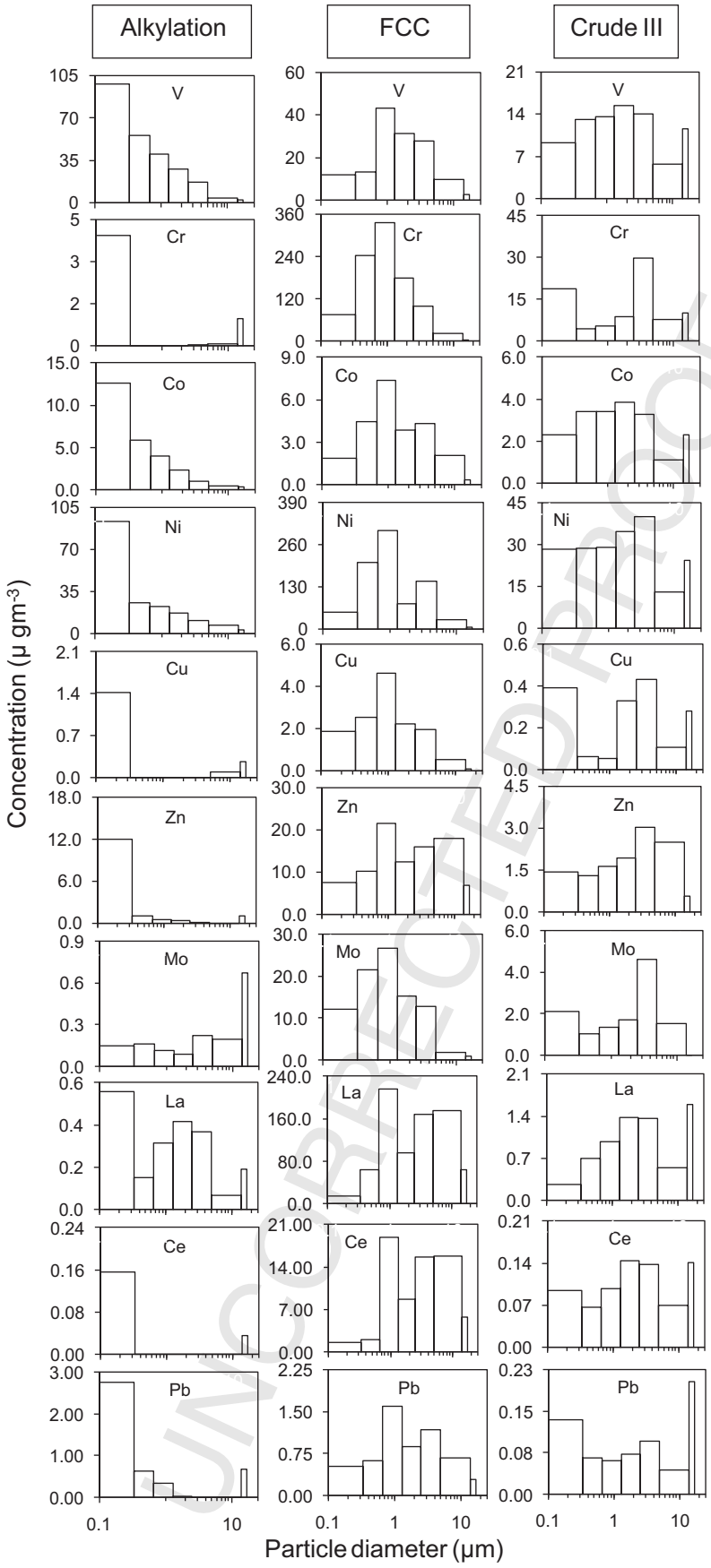

Fig. 4. Concentration and particle size distribution from alkylation, FCC and Crude IIII process of FCC and Crude III plant.

Please cite this article in press as: A.M. Sánchez de la Campa, et al., Size distribution and chemical composition of metalliferous stack emissions in the San Roque petroleum refinery complex, southern Spain, J. Hazard. Mater. (2011), doi:10.1016/j.jhazmat.2011.03.104

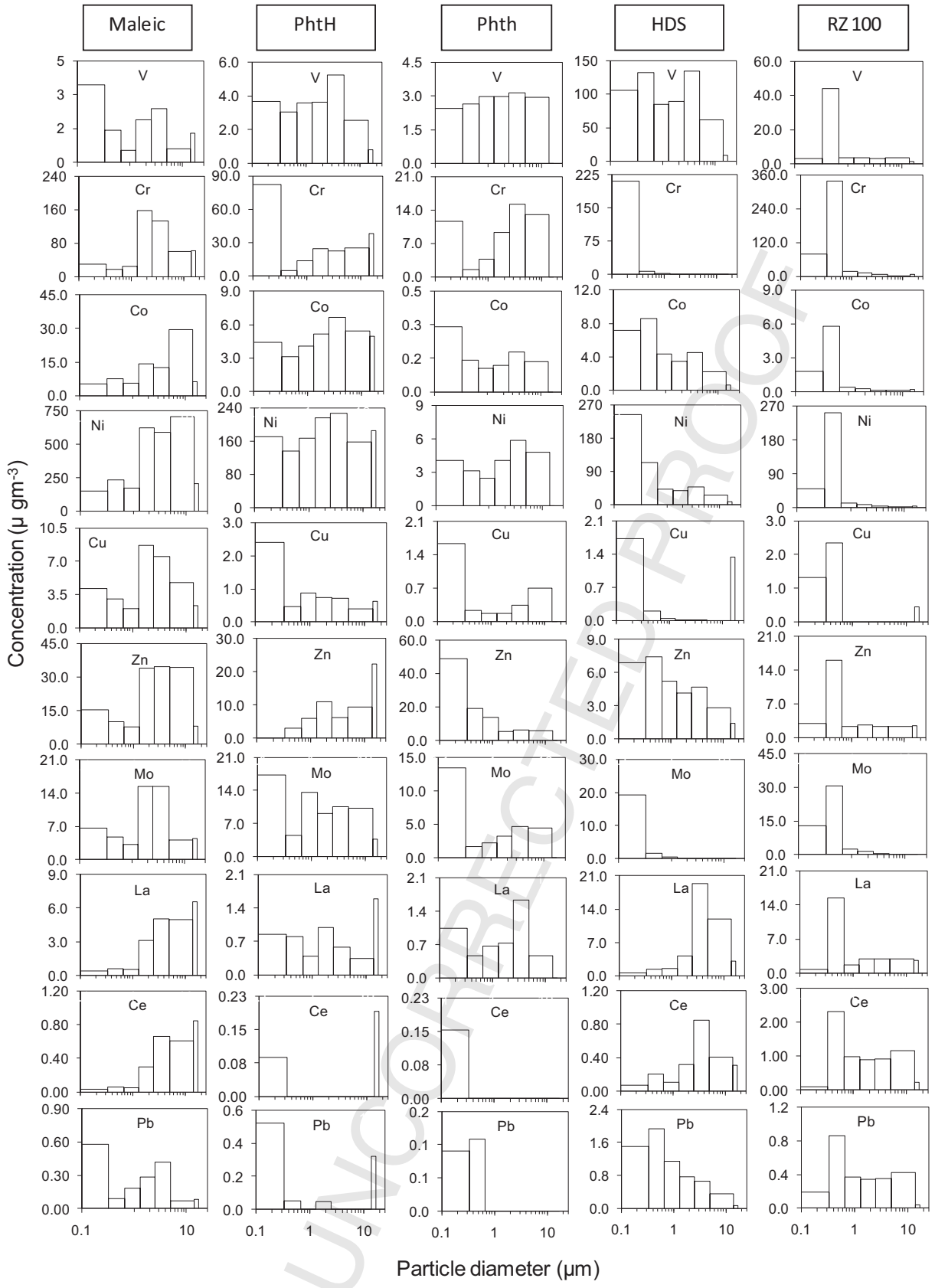

Fig. 5. Concentration and particle size distribution from Maleic, High combustion Phthalic (PhtH), Habitual combustion Phthalic (Phth) HDS and RZ 100 process of Guadarranque plant.

Please cite this article in press as: A.M. Sánchez de la Campa, et al., Size distribution and chemical composition of metalliferous stack emissions in the San Roque petroleum refinery complex, southern Spain, J. Hazard. Mater. (2011), doi:10.1016/j.jhazmat.2011.03.104

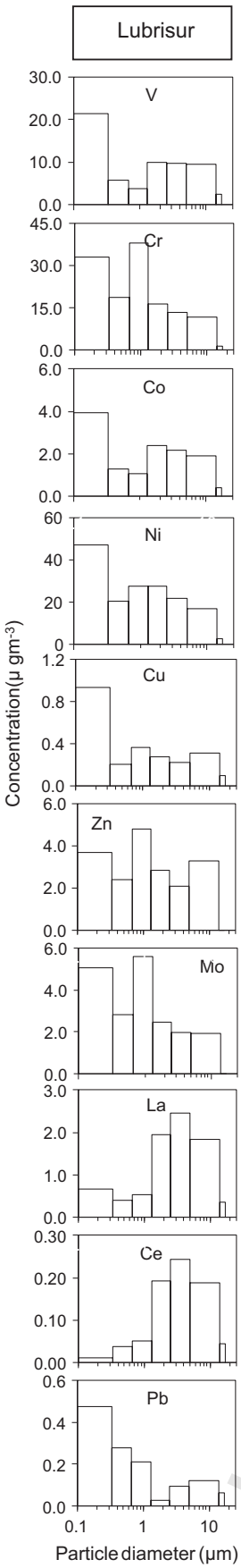

Fig. 6. Concentration and particle size distribution of Lubrisur plant.

($70\,\mu g\,m^{-3}$) and Zn ($70\,\mu g\,m^{-3}$) in the combustion sample; Ni ($367\,\mu g\,m^{-3}$), Cr ($240\,\mu g\,m^{-3}$), and V ($85\,\mu g\,m^{-3}$) in the sulpholane sample; and V ($70\,\mu g\,m^{-3}$), Ni ($44\,\mu g\,m^{-3}$) and Cr ($25\,\mu g\,m^{-3}$) in the Crude I sample.

Of the three samples from the *FCC plant* (alkylation, FCC and Crude III) the size distribution profiles of the alkylation sample are similar to those of the combustion and sulpholane samples of the combustion plant (Fig. 4). The sample obtained specifically from the FCC unit is characterised by an unimodal size distribution (maximum concentration reached intermediately between the fine to coarse modes) for V + Cr + Co + Ni + Cu + Mo, and a bimodal shape profile (fine and coarse size modes) in La, Ce, Zn and Pb. In contrast, in the Crude III sample size distribution profiles have no clear pattern, due to the low emission concentrations close to the analytical lower detection limit. The highest metal emission concentrations in these three chimneys were registered by Ni ($302\,\mu g\,m^{-3}$), Cr ($336\,\mu g\,m^{-3}$) and La ($215\,\mu g\,m^{-3}$) in the FCC sample, V ($98\,\mu g\,m^{-3}$) and Ni ($93\,\mu g\,m^{-3}$) in the alkylation sample, and Ni ($40\,\mu g\,m^{-3}$) Cr ($30\,\mu g\,m^{-3}$) in the Crude III sample.

The size distributions of the elemental mass concentrations of *Guadarranque plant* samples (RZ 100, HDS, Phth and PhtH, Maleic) are summarized in Fig. 5. The major constituent elements are Ni + Cr + V + Zn + Co + Mo and La, and both unimodal and bimodal size distributions are evident. With regard to the unimodal patterns, three main size ranges have been distinguished: ultrafine, fine and coarse. Ultrafine (<0.33 μm) is characterised by a maximum concentration of Cr + Co + Ni + Cu + Mo + Pb in the HDS sample, Zn + Mo + Ce + Pb in the Phth sample, and Cu in the PhtH sample. Maximum concentrations of V + Cr + Co + Ni + Cu + Zn + Mo + La + Ce + Pb in the RZ100 sample are recorded in the fine size distribution (0.33–0.67 μm), whereas PM in the coarse size range (>2.5 μm) with a unimodal pattern show maximum concentrations of Cr + Co + Ni + Cu + Zn + Mo + La + Ce in the Maleic sample, Zn + La + Ce in the PhtH sample, La in the at Phth sample, and La + Ce in the HDS sample. Bimodal distribution exhibits both ultrafine (<0.33 μm) and coarse (>2.5 μm) modes, with enrichments in V + Pb (Maleic), Cr (PhtH), and Cr + Co + Ni + Cu (Phth). The highest metal emission concentrations in these five Guadarranque samples were registered by Cr ($339\,\mu g\,m^{-3}$) and Ni ($252\,\mu g\,m^{-3}$) in the RZ100 sample, Ni ($244\,\mu g\,m^{-3}$) and Cr ($211\,\mu g\,m^{-3}$) in the HDS sample, Zn ($49\,\mu g\,m^{-3}$) and Cr ($15\,\mu g\,m^{-3}$) in the Phth sample, Ni ($227\,\mu g\,m^{-3}$) and Cr ($83\,\mu g\,m^{-3}$) in the PhtH sample, and Ni ($713\,\mu g\,m^{-3}$) and Cr ($157\,\mu g\,m^{-3}$) in the Maleic sample.

In contrast to the previously described samples, those from the *Lubrisur plant* (Fig. 6) did not show a strongly distinctive size distribution pattern. However, there is a bimodal distribution (ultrafine and coarse sizes) with a maximum concentration of V + Cr + Co + Ni + Pb, and a unimodal distribution of La + Ce.

Table 1 summarizes relevant elements and size grain modes (ultrafine-fine, fine-coarse and coarse) of the stacks emission particles at San Roque Refinery, and clarifies the high diversity of size mode and chemistry between the samples. The unimodal and bimodal grain size distributions imply that elements present in emission particles are controlled by several processes. Most of the analysed units are enriched in metals (e.g. V + Cr + Co + Ni + Cu + Zn + Mo) in the ultrafine-fine size mode, this being attributed to the combustion of petroleum derived products, and proportionally higher from a contaminating effect of tubepipe line erosion [19]. However, FCC emission are clearly more enriched in V + Cr + Co + Ni + Cu + Mo and La + Ce + Zn in fine to coarse particles, respectively, compared to other units. This bimodality is interpreted as resulting from a mixing of fine particles from petroleum combustion and coarser PM escaping from the FCC catalyst [14,15,20–22].

Please cite this article in press as: A.M. Sánchez de la Campa, et al., Size distribution and chemical composition of metalliferous stack emissions in the San Roque petroleum refinery complex, southern Spain, J. Hazard. Mater. (2011), doi:10.1016/j.jhazmat.2011.03.104

Table 2
Chemical composition of sampled unit stacks.

Production area	CEA			FCC			Guadarranque					Lubrisur	Total
Unit	Combustion	Sulpholane	Crude I	Alkylation	FCC	Crude III	RZ-100	HDS	Phtalic h	Phtalic H	Maleic	Lubrisur	
Flow (Nm^3/h)	154,100	173,200	537,000	8000	154,400	87,400	71,700	39,900	3600	23,400	35,700	81,000	
Temperature (°C)	278	263	221	358	234	291	174	249	633	271	40	99	
Volume (Nm^3)	0.52	0.75	0.99	0.53	0.69	0.53	0.97	1.06	0.56	0.56	1.13	0.88	9.17
Concentration ($mg\,m^{-3}$)	18.0	37.6	47.0	33.6	261	3.6	27.4	37.0	59.3	33.0	129	7.50	694
$\mu g\,m^{-3}$													
Li	0.16	5.72	0.13	7.83	3.47	0.12	1.36	0.15	1.21	8.01	0.81	0.09	29.1
Be	0.06	0.10	0.04	0.11	0.15	0.02	0.02	0.05	0.01	0.05	0.01	0.01	0.64
Sc	0.05	0.62	0.33	<0.01	0.49	0.01	0.01	0.14	0.00	0.00	0.02	0.00	1.68
V	140	210	203	253	145	85.9	66.9	638	19.90	25.1	14.5	64.3	1866
Cr	53.2	406	34.9	5.04	962	94.6	476	225	57.7	270	568	144	3296
Co	18.3	16.7	9.53	27.0	24.8	20.3	9.23	31.7	1.10	40.8	93.9	13.6	307
Ni	187	526	160	182	819	208	344	526	26.1	1522	3295	173	7969
Cu	5.77	7.77	0.84	2.06	14.0	1.73	4.12	3.31	4.02	6.96	36.7	2.52	89.8
Zn	108	45.7	29.7	20.0	98.7	14.5	34.2	35.6	117	105	225	21.8	855
Ga	1.24	0.84	1.55	1.15	3.31	0.12	0.40	2.99	<0.01	<0.01	0.27	0.25	12.1
Ge	0.13	0.10	0.04	0.03	0.89	0.05	0.11	0.07	0.08	0.08	0.24	0.06	1.85
As	1.96	1.13	0.72	1.62	1.63	0.76	0.43	1.47	0.16	0.15	0.54	0.75	11.3
Se	0.35	0.79	0.28	0.64	0.58	0.63	0.24	0.53	0.11	0.13	1.00	0.64	5.92
Rb	0.22	1.20	0.19	0.03	0.68	0.10	0.04	0.11	0.01	0.06	6.56	0.05	9.25
Sr	1.81	7.36	0.95	1.71	1.74	1.06	0.93	1.87	0.23	0.20	10.8	1.22	29.9
Y	1.58	0.67	1.00	0.31	2.22	0.11	0.55	0.54	0.08	0.00	0.10	0.09	7.24
Zr	1.82	31.7	0.17	1.69	31.8	0.29	0.83	0.87	1.04	0.67	5.86	2.08	78.8
Nb	1.38	0.98	0.59	0.11	2.91	0.14	0.87	0.43	0.12	0.34	0.68	0.21	8.76
Mo	10.0	33.2	4.50	1.97	91.1	13.84	48.7	21.6	31.5	82.1	66.6	22.2	427
Cd	3.68	0.59	0.18	0.11	2.92	0.04	0.57	0.10	0.1	0.61	2.10	0.07	11.0
Sn	0.21	0.42	0.14	0.18	0.92	0.24	0.26	0.17	0.11	0.40	0.40	0.08	3.53
Sb	0.43	0.35	0.08	0.99	0.41	0.34	0.01	0.37	0.32	0.21	0.29	0.24	4.02
Cs	0.00	0.22	0.00	0.09	0.04	0.33	0.00	0.00	0.01	0.09	0.06	0.00	0.85
Ba	61.3	50.3	56.5	14.2	36.3	2.51	25.5	87.0	0.79	0.00	12.4	3.54	350
La	19.7	13.54	40.9	5.03	865	7.28	41.1	46.7	5.55	6.13	28.0	8.82	1088
Ce	8.43	1.18	1.57	1.94	76.3	0.80	8.63	2.50	0.15	0.28	3.46	0.84	106
$\sum$ REE	36.53	21.37	51.78	8.59	1058.7	9.59	59.98	58.25	6.14	7.75	37.99	11.29	1368
Hf	0.45	0.57	0.24	0.07	0.63	0.03	0.06	0.16	0.11	0.08	0.23	0.06	2.70
Ta	0.00	0.32	0.03	0.26	0.22	0.02	0.00	0.02	0.11	0.19	0.01	0.01	1.20
W	0.21	1.14	0.09	0.08	1.50	0.19	1.10	0.31	0.23	0.91	1.83	0.31	7.89
Tl	0.00	0.39	0.00	0.00	0.10	0.04	0.00	0.00	0.00	0.00	0.07	0.03	0.63
Pb	7.89	5.58	4.99	5.25	6.41	0.73	3.00	6.84	0.24	1.31	2.13	1.34	45.7
Bi	0.00	0.01	0.00	0.00	0.00	0.04	0.00	0.00	0.00	0.00	0.01	0.02	0.08
Th	5.70	1.05	1.68	0.97	2.14	0.03	3.28	1.86	0.04	0.00	0.02	0.03	16.8
U	0.14	0.36	0.14	0.05	0.55	0.04	0.02	0.07	0.06	0.08	0.03	0.02	1.55

Please cite this article in press as: A.M. Sánchez de la Campa, et al., Size distribution and chemical composition of metalliferous stack emissions in the San Roque petroleum refinery complex, southern Spain, J. Hazard. Mater. (2011), doi:10.1016/j.jhazmat.2011.03.104

5. Discussion and conclusions

The evaluation of the experimental chemical data on metal emissions at the San Roque refinery (Table 2) suggests that the highest concentrations averaged over all size ranges were registered in the following decreasing order: Ni (up to 3295 $\mu g\,m^{-3}$) > Cr (962 $\mu g\,m^{-3}$) > La (865 $\mu g\,m^{-3}$) > V (638 $\mu g\,m^{-3}$) > Zn (225 $\mu g\,m^{-3}$) > Co (94 $\mu g\,m^{-3}$) > Mo (91 $\mu g\,m^{-3}$). The combustion unit emitted with the highest concentrations of Zn, As and Cd, the sulpholane unit with the highest Se, Sr and Pb, the FCC unit produced the highest concentrations in Cr, Ga, Zr, Mo and REE, whereas Sb and Li emission levels were highest in the alkylation unit. Finally the different stacks in the Guadarraque plants (Fig. 5) emitted especially high concentrations of V (HDS unit), Cr and Mo (RZ-100 unit), and Co, Ni, Cu and Rb (Maleic unit).

The high concentrations of ambient metals recorded in PM_{10} and $PM_{2.5}$ from representative monitoring stations of the Bay of Algeciras have been attributed in part to emissions from the San Roque refinery [14]. In particular, according to Moreno et al. [14], high concentrations of V (28 $ng\,m^{-3}$), Cr (25 $ng\,m^{-3}$), Ni (20 $ng\,m^{-3}$) and La (0.58 $ng\,m^{-3}$) are present within ambient atmospheric PM_{10} in the Algeciras area. Although the exact size ranges of these ambient particles remains unstudied, these authors further note that the metalliferous aerosols typically are extremely fine in size and therefore potentially bioavailable, making a clear case for basing urban background PM characterisation not only on physical parameters such as mass but also on sample chemistry and with special emphasis on trace metal content. The data presented here confirms that many metals are indeed present in high concentrations in the refinery complex chimney stacks, with exceptional concentrations of >100 $\mu g\,m^{-3}$ being reached by V, Cr, Ni, and La. These extreme levels are not uniformly emitted but focused on specific stacks within the petrochemical complex. Taking each of these four metals in turn, in the case of *Vanadium* the highest concentrations are found within emissions from the HDS unit in the Guadarranque plant and from the alkylation, sulpholane, combustion, and Crude I units (Figs. 3–5). A clear difference between these diverse sources is that whereas the HDS unit emits abundant V-rich PM in all sizes ranging up to PM10 (Fig. 5), all the other four sources emit mostly very fine PM (<0.33 μm). *Chromium*-rich PM measured in the stack samples is most abundant in the RZ-100 and HDS units of the Guadarranque plant and in the FCC and sulpholane units (Figs. 3–5). Most of these Cr-rich PM are once again fine in size (<0.5 μm), although the FCC unit shows a broader size range peaking around 1 μm. With respect to *Nickel*-rich PM, these are highly abundant in six of the stack samples, especially in the Maleic and sulpholane units, but also in the FCC, PhtH, HDS and RZ-100 units. Once again, although many of the NiPM are very fine in size, some units show a very broad size range (FCC, PhtH: Figs. 4 and 5). Finally, the most spectacular point source contamination of all the metals analysed is that displayed by *Lanthanum* in the FCC unit, with concentrations exceeding 200 $\mu g\,m^{-3}$ and a relatively coarse size distribution of (1–10 μm) confirming derivation from the La-rich catalyst.

Of the 12 samples analysed it is clear the stacks producing the highest concentrations of metalliferous particles are those associated with the following 8 units: combustion (high V, Ni, Zn < 0.33 μm), sulpholane (high V, Cr, Ni < 0.33 μm), Crude I and alkylation (high V < 0.33 μm), FCC (high Cr, Ni, La (0.3–10 μm), Maleic (high Ni, Co 1–10 μm), HDS (V < 10 μm, Cr and Ni < 0.33 μm, La 2–10 μm), and RZ-100 (Cr, Ni, Mo 0.3–0.7 μm. In contrast, relatively low metalliferous concentrations are found in the Crude III and Lubrisur stacks (Figs. 4 and 6).

Most of the more toxic metals concentrate in the finer PM sizes in most samples, reinforcing the visual observations provided by the SEM data (Fig. 2). Thus PM escaping into the atmosphere from these refinery complex stacks will be capable of both proximal and distal contamination, and individual particles will be small enough to be easily inhaled into the deep lung environment [23]. The Bay of Algeciras has consistently presented higher than average rates of cancer incidence and mortality, comprising one of the vertices of a triangle centred between the provinces of Huelva, Cádiz and Seville and contaminated by a range of industrial emissions [10,24–27]. If this increased health risk is linked to air pollution from the refinery complex, then it is the metalliferous component of the emissions which is likely to be at least part of the problem. It clear from our unique database that there is great chemical and size variation in the cocktail of metalliferous pollutants emanating from different emission stacks in refinery complexes, and that some point sources are considerably more contaminating and potentially toxic than others.

Acknowledgments

This study was supported by the Department of the Environment and the Department of Innovation, Science and Enterprise (project RNM2007-02729) of the Autonomous Government of Andalusia, and Projects GRACCIE-CSD2007 of the Spanish Ministry of Science and Innovation. The authors are indebted to Juan Contreras, Francisca Godoy and Antonio Lozano of the Department of Air Quality in the Environmental Office of Andalusia Government for their collaboration with this study. Thanks are due to Wes Gibbons for his revision of the manuscript.

References

[1] C. Riccardi, P. Di Filippo, D. Pomata, F. Incoronato, M. Di Basilio, M.P. Papini, S. Spicaglia, Characterization and distribution of petroleum hydrocarbons and heavy metals in groundwater from three Italian tank farms, Science of The Total Environment 393 (2007) 50–63.
[2] F. Korte, E. Boedefeld, Ecotoxicological review of global impact of petroleum industry and its products, Ecotoxicology and Environmental Safety 2 (1978) 55–103.
[3] A.N. Garg, N.L. Chutke, M.N. Ambulkar, R.K.S. Dogra, An evaluation of the environmental implications of petroleum refinery emissions by multielemental neutron activation analysis of rumen fluid ash of buffaloes, Applied Radiation and Isotopes 47 (1996) 581–586.
[4] I.N. Luginaah, S.M. Taylor, S.J. Elliott, J.D. Eyles, A longitudinal study of the health impacts of a petroleum refinery, Social Science and Medicine 50 (2000) 1155–1166.
[5] P.A. Bertazzi, A.C. Pesatori, C. Zocchetti, R. Latocca, Mortality study of cancer risk among oil refinery workers, International Archives of Occupational and Environmental Health 61 (1989) 261–270.
[6] T.L. Terry, P. Decoufle, R. Moure-Eraso, Mortality among workers employed in petroleum refining and petrochemical plants, Journal of Occupational and Environmental Medicine 22 (1980) 97–103.
[7] C.Y. Yang, B.H. Chen, T.Y. Hsu, S.S. Tsai, C.F. Hung, T.N. Wu, Female lung cancer mortality and sex ratios at birth near a petroleum refinery plant, Environmental Research 83 (2000) 33–40.
[8] S. Belli, M. Benedetti, P. Comba, D. Lagravinese, V. Martucci, M. Martuzzi, D. Morleo, S. Trinca, G. Viviano, Case–control study on cancer risk associated to residence in the neighbourhood of a petrochemical plant, European Journal of Epidemiology 19 (2004) 49–54.
[9] N. Simonsen, R. Scribner, L.J. Su, D. Williams, B. Luckett, T. Yang, E.T.H. Fontham, Environmental exposure to emissions from petrochemical sites and lung cancer: the lower Mississippi Interagency Cancer Study, Journal of Environmental and Public Health (2010) 9, Article ID 759645.
[10] J. García-Pérez, E. Boldo, R. Ramis, M. Pollán, B. Pérez-Gómez, N. Aragonés, G. López-Abente, Description of industrial pollution in Spain, BMC Public Health 7–40 (2007) 1–13.
[11] X. Querol, M. Viana, A. Alastuey, F. Amato, T. Moreno, S. Castillo, J. Pey, J. de la Rosa, A. Sánchez de la Campa, B. Artinano, P. Salvador, S. Garcia Dos Santos, R. Fernandez-Patier, S. Moreno-Grau, L. Negral, M.C. Minguillon, E. Monfort, J.I. Gil, A. Inza, L.A. Ortega, J.M. Santamaria, J. Zabalza, Source origin of trace elements in PM from regional background, urban and industrial sites of Spain, Atmospheric Environment 41 (2007) 7219–7231.
[12] J.D. de la Rosa, A.M. Sánchez de la Campa, A. Alastuey, X. Querol, Y. González Castanedo, R. Fernández Camacho, A.F. Stein, Using geochemical maps in PM_{10} defining the atmospheric pollution in Andalusia (Southern Spain), Atmospheric Environment 44 (2010) 4595–4605.
[13] M. Pandolfi, Y. González-Castanedo, A. Alastuey, J.D. de la Rosa, E. Mantilla, A. Sánchez de la Campa, X. Querol, J. Pey, F. Amato, T. Moreno, Source apportionment of PM_{10} and $PM_{2.5}$ at multiple sites in the Strait of Gibraltar by PMF:

impact of shipping emissions, Environmental Science and Pollution Research (2010). doi:10.1007/s11356-010r-r0373-4.
[14] T. Moreno, X. Querol, A. Alastuey, J.D. de la Rosa, A.M. Sánchez de la Campa, M.C. Minguillón, M. Pandolfi, Y. González-Castanedo, E. Monfort, W. Gibbons, Variations in vanadium, nickel and lanthanoid element concentrations in urban air, Science of the Total Environment 408 (2010) 4569–4579.
[15] M.E. Kitto, D.L. Anderson, G.E. Gordon, I. Olmez, Rare Earth distributions in catalysts and airbonrne particles, Environmental Science and Technology 26 (1992) 1368–1375.
[16] P. Kulkarni, S. Chellam, M. Fraser, Lanthanum and lanthanides in atmospheric fine particles and their apportionment to refinery and petrochemical operations in Houston, TX, Atmospheric Environment 40 (2006) 508–520.
[17] M.J. Pilat, D.S. Ensor, J.C. Bosch, Source test cascade impactor, Atmospheric Environment 4 (1970) 671–679.
[18] X. Querol, A. Alastuey, S. Rodriguez, F. Plana, C.R. Ruiz, N. Cots, G. Massague, O. Puig, PM_{10} and $PM_{2.5}$ source apportionment in the Barcelona metropolitan area, Catalonia, Spain, Atmospheric Environment 35 (2001) 6407–6419.
[19] J.C. Groen, J.R. Craig, The inorganic geochemistry of coal, petroleum, and their gasification/combustion products, Fuel Processing Technology 40 (1994) 15–48.
[20] P. Kulkarni, S. Chellam, M.P. Fraser, Tracking petroleum refinery emission events using lanthanum and lanthanides as elemental markers for $PM_{2.5}$, Environmental Science and Technology 41 (2007) 6748–6754.
[21] T. Moreno, X. Querol, A. Alastuey, W. Gibbons, Identification of FCC refinery atmospheric pollution events using lanthanoid- and vanadium-bearing aerosols, Atmospheric Environment 42 (2008) 7851–7861.
[22] T. Moreno, X. Querol, A. Alastuey, J. Pey, M.C. Minguillón, N. Pérez, R.M. Bernabé, S. Blanco, B. Cárdenas, W. Gibbons, Lanthanoid geochemistry of urban atmospheric particulate matter, Environmental Science and Technology 42 (2008) 6502–6507.
[23] B. Brunekreef, S.T. Holgate, Air pollution and health, The Lancet 360 (2002) 1233–1242.
[24] J. Benach, Y. Yasui, C. Borrell, E. Rosa, M.I. Pasarín, N. Benach, E. Español, J.M. Martínez, A. Daponte, Examining geographic patterns of mortality. The Atlas of mortality in small areas in Spain (1987–1995), European Journal of Public Health 13 (2003) 115–123.
[25] J. Benach, Y. Yasui, J.M. Martínez, C. Borrel, M.I. Pasarín, A. Daponte, The geography of the highest mortality areas in Spain: a striking cluster in the southwestern region of the country, Occupational and Environmental Medicine 61 (2004) 280–281.
[26] G. López-Abente, N. Aragonés, R. Ramis, V. Hernández-Barrera, B. Pérez-Gómez, A. Escolar-Pujolar, M. Pollant, Municipal distribution of bladder cancer mortality in Spain: possible role of mining and industry, BMC Public Health 6–17 (2006) 1–10.
[27] C. Cruz Rojo, M. Almisas, Epidemiological analysis of mortality by causes in Bahía de Algeciras, Spain (2001–2005), Gaceta Sanitaria 5 (2009) 388–395.

Please cite this article in press as: A.M. Sánchez de la Campa, et al., Size distribution and chemical composition of metalliferous stack emissions in the San Roque petroleum refinery complex, southern Spain, J. Hazard. Mater. (2011), doi:10.1016/j.jhazmat.2011.03.104